Biol Cybern (2008) 98:509–518
DOI 10.1007/s00422-008-0215-3

ORIGINAL PAPER

Biological Cybernetics

Population vector code: a geometric universal as actuator

J. Leo van Hemmen · Andrew B. Schwartz

Received: 17 January 2008 / Accepted: 30 January 2008

Abstract The population vector code relates directional tuning of single cells and global, directional motion incited by an assembly of neurons. In this paper three things are done. First, we analyze the population vector code as a purely geometric construct, focusing attention on its universality. Second, we generalize the algorithm on the basis of its geometrical realization so that the same construct that responds to sensation can function as an actuator for behavioral output. Third, we suggest at least a partial answer to the question of what many maps, neuronal representations of the outside sensory world in space–time, are good for: encoding vectorial input they enable a direct realization of the population vector code.

Keywords Assembly · Population · Population vector · Population vector code · Muscles · Actuator

1 Introduction

When an animal "observes" a stimulus, viz., predator, prey, or conspecific, moving in space–time its neuronal processing can be decomposed into at least three components. First, stimulus action has to be observed physically by detectors such as retinal or infrared cells, or mechanosensory cells in the auditory or lateral-line system in passive localization. Alternatively, there is active localization as performed by bats, blind Mexican cave fish, or weakly electric fish. The ensuing neuronal action leads to object formation and localization. The neuronal "object" is to characterize the stimulus in terms of the sensorty modality/ies involved whereas "localization" is performed through a *map*, a neuronal representation of the outside sensory world (van Hemmen 2006). Both passive and active detection constitute action in space–time, i.e., space *and* time—in agreement with the spatio-temporal nature of their input.

Second, the map or several maps arising from sensory input is, or are, transformed into some representation that can be acted on by the motor system. We will skip multisensory integration, exciting as it may be.

Third, and finally, the motor system expresses behavior as an "actuator" and generates an output through muscular action. This is what we focus on first.

Signs of the fascinating actuator in this story were discovered in the mid eighties of last century in the activity of motor cortical neurons (Georgopoulos et al. 1982, 1983, 1986). The underlying geometric idea is appealingly simple and its predictions are extremely powerful. Let us assign to each neuron with label i its *preferred direction* $\boldsymbol{e}_i$, a unit vector. For an assembly (Hebb 1949) or population of motor neurons $\{1 \leq i \leq N\}$ with momentary firing rate ν_i the weighted vector sum, the so-called *population vector* $\boldsymbol{n}$,

$$\boldsymbol{n} := \nu \boldsymbol{e} = \sum_{i=1}^{N} \nu_i \, \boldsymbol{e}_i \tag{1}$$

encodes the direction $\boldsymbol{e}$ of movement resulting from an assembly of motor neurons while ν, the length of the population vector $\boldsymbol{n}$, is proportional to the instantaneous speed of the drawing motion we focus on. In passing we note that the instantaneous firing rate ν_i measures the momentary activity of neuron i.

J. L. van Hemmen (✉)
Physik Department, TU München,
85747 Garching bei München, Germany
e-mail: lvh@tum.de

A. B. Schwartz
Motor Lab, School of Medicine,
University of Pittsburgh,
Pittsburgh, PA 15261, USA

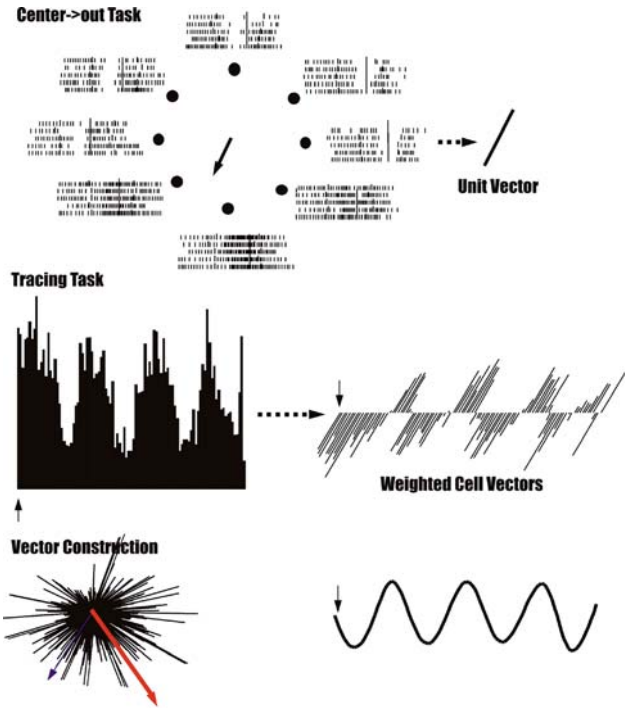

Fig. 1 Calculation of population vectors. *Top row* The preferred direction of each cell is found from the so-called center → out task. Rasters show when the cell fired relative to movement onset (long tick is movement onset, one row of tick marks for each trial, horizontal axis is time aligned to movement onset, rasters arranged by movement direction). A unit vector represents the cell's preferred direction. *Middle row* In this example, the monkey drew a sinusoid and the activity of the recorded neuron was highly modulated, increasing its discharge rate every time the finger movement moved downward. The rates are plotted in the histogram on the left, the rate in each bin is used to weight the cell vector pointing in the preferred direction. A weighted cell vector is calculated for each bin. The *small arrow* marks the first bin. *Bottom row* The first weighted cell vector from the example cell is represented by the arrow in the cluster on the left pointing in bottom-left direction. The same experiment is carried out hundreds of times while recording from different cells. Each of those cells also contributes a weighted cell vector (black vectors, here simple lines, in cluster). These are all summed to produce the population vector (*big arrow*). This represents the trajectory in the first bin of the movement as shown by the neural trajectory on the right which is constructed by adding population vectors from subsequent bins tip-to-tail

The above statements are purely experimental facts and we accept them as constituting a natural law, which simply means a mathematical formulation of experimental findings that is known under the name of 'population vector code' or as we prefer to call it, the 'population vector algorithm'; see Fig. 1 for an experimental illustration. It is a very potent algorithm, indicating how a movement, even a continuous one, can be represented by an assembly of neurons. That is, we accept it as such and do not attempt at all to derive it. In a sense, we see the population vector algorithm (PVA) as a general principle describing movement representation. However the brain really works, it must contain properties that allow us to make good predictions using the algorithm embodied in the population vector. There is no physical instantiation of the population vector per se. This would require a summing node that is unlikely to exist. The summation probably does not happen until all the muscles contract in their special way to move the limb.

Assembly and population codes have long histories. Donald Hebb in his classic *The organization of behavior* (Hebb 1949) was the first to stress the relevance of what he called an 'assembly' of neurons to encode or decode information. As for the population vector code, there are many references, some interesting, some learned, some mathematically challenging, but nearly all focusing on the statistics of the population. We refer to a few (Salinas and Abbott 1994; Lewis 1999; Averbeck et al. 2006) for an extensive overview incl. references, and focus here on the *geometrical* nature of the population vector algorithm and the function of the population in generating motor behavior.

In the next section, we treat the population vector algorithm proper. We then analyze and generalize its role as neuronal actuator, and finish our essay by suggesting an at least partial answer to one out of a collection of 23 key problems in systems neuroscience (van Hemmen and Sejnowski 2006): What is a neuronal map good for?

2 Population vector algorithm generating motion

Cosine tuning of individual neuronal responses is the basic factor underlying the success of the population vector algorithm (PVA); see Fig. 2. In the original discovery (Georgopoulos et al. 1982), monkeys moved their arms from the center of a surface to eight targets evenly spaced in a circle around the start position. The modulation of neuronal activity recorded from the motor cortex in this task was specific to the direction of the reach. Neurons tended to fire at some maximal rate in a single direction (preferred direction) and fire at progressively lower rates at larger angles away from this. Tuning functions were constructed by plotting the average discharge rate to each target against the direction of the target from the center start position. These data were fit with a simple multiple regression model expressed as a cosine function between direction and discharge rate; we call this fit *cosine tuning*. Most of the motor-cortical neurons recorded in this task had tuning functions that were significantly fit by a cosine.

The cosine functions have a period of 2π, suggesting that these neurons are modulated by all movement directions. Conversely, during every movement, most of the neurons in the motor cortex are modulated simultaneously. A large population of neurons is active at the same time throughout all movements. Furthermore, for the cosine function itself there is a nice hindsight argument based on Fisher information (Zhang and Sejnowski 1999).

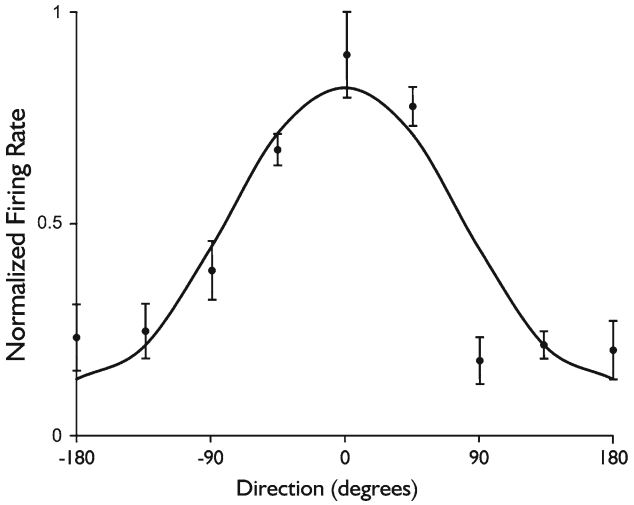

Fig. 2 Cosine tuning function. Discharge rate versus movement direction in the center-out task. The rate of an individual neuron (normalized, min = 0, max = 1). Movement direction is the angle from the cell's preferred direction (the movement direction with the highest discharge rate). Data are mean and standard deviation of discharge rates from five trials of movements to each of eight targets. The cosine function was fit by a linear regression of the direction to the firing rate for the experiment of Fig. 1, *top row*

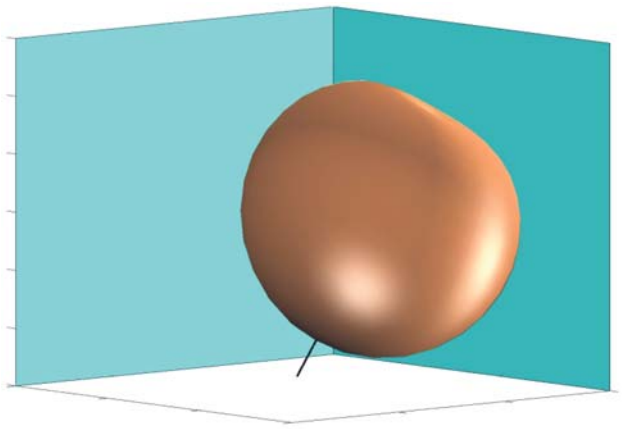

Fig. 3 3-Dimensional tuning function. This shows what a tuning function looks like in three-dimensional Cartesian space. The origin is at the dimple on the upper right side of the volume. The distance from the origin to the shell in the direction of movement is proportional to the firing rate of a cosine-tuned neuron. The vector emerging from the bottom is pointing in the cell's preferred direction

Decoding, in this context, can be defined as a mapping between neuronal activity and movement direction. Although tuning functions of individual cells provide this mapping, they function poorly as a decoding device. Each discharge rate corresponds to two points (and two directions) on the tuning curve. In addition, the discharge rates used for this mapping are noisy so that there is a large uncertainty in this mapping.

The solution for decoding lies in the consideration of a *population* or, as Hebb (1949) called it, an assembly of neuronal responses. Georgopoulos et al. (1984) developed the PVA as a way of extracting movement direction from a population of tuned neurons. Each neuron's contribution was represented as a vector oriented in that cell's preferred direction. The vector's length was proportional to the mean firing rate of the neuron during movement to the target under consideration. Contributions from the recorded population of tuned neurons were added together *vectorially* and the resultant *population vector* pointed in and predicted the movement direction; cf. Eq. (1). As is illustrated by Fig. 3, his algorithm was subsequently extended to three dimensions (Georgopoulos et al. 1986, 1988; Schwartz et al. 1988), drawing movements (Schwartz 1994), and prosthetic control (Taylor et al. 2002). Population vectors *continuously* represent the instantaneous velocity of e.g. the hand and this allows for an isomorphic extraction of the arm's trajectory from cortical activity.

The success of the population vector algorithm depended on two major factors: the cosine-like behavior of individual neurons and the uniformity of the preferred direction distribution across the population (Seung and Sompolinsky 1993; Salinas and Abbott 1994) in a great variety of systems such as spinocerebellar neurons (Bosco and Poppele 1993), the superior colliculus (Kutz et al. 1997), cerebellum (Johnson and Ebner 2000), basal ganglia (Turner and Anderson 1997), and parietal cortex (Kalaska et al. 1983; Motter et al. 1987). One idea about this robust representation is that the cosine function may be representative of correlation. The similarity between two vectors of arbitrary dimensionality is proportional to the cosine of the angle between them. The cosine-like tuning of these many neurons may be indicative of the way inputs to these cells are combined and/or the operation being performed on them.

One goal of cortical neurophysiologists is to identify and describe the mechanics of a cortical 'operation' (Mountcastle 1998). Generation of cosine tuning functions may be more intermediate since cosine tuning is prevalent throughout the motor system. Transformation of inputs to cells that are sinusoidally tuned, could be straightforward in terms of correlation to cosine-like output. The cortical operation concept may be broadened to include the sort of transformations that take place in the generation of volitional movement.

An example of this is the mapping between coordinate systems (Pellionisz 1988; Helms Tillery et al. 1991; Soechting and Flanders 1991b) and the fact that muscles must act across joints. It has generated a lot of controversy that still persists (Schwartz 2007). However, even though there are more degrees of freedom in the intrinsic space, arm movements are generated with strategies that link multiple joints together (Soechting 1989; Soechting and Flanders 1991a). When cortical activity regression was compared to models based on hand velocity (extrinsic) and joint angular velocity (intrinsic),

both models appeared to be equally valid, showing that both coordinate frames were correlated (Reina et al. 2001). Generating movement based on correlation between reference frames is an efficient strategy that would obviate explicit transformation. Of course, this process is not limited to the cortex and likely spans the entire neuroaxis, a concept that matches the finding of wide-spread cosine tuning.

3 Population vector algorithm as neuronal actuator

A natural question therefore is: does the above algorithm hold only for motor systems or is it a more general geometrical procedure to mathematically describe how animals move in space and time? Here we will argue that there is a lot of evidence pointing exactly in this direction. That is to say, the population vector algorithm is effectively a neuronal actuator transforming neuronal activity into action. We will illustrate our general statement through a detailed analysis of the neurobiology of the sand scorpion's detection and response to prey, an example so simple that it allows a full comprehension of all computational steps. In addition, we will show that the back swimmer's prey localization can be described by the very same algorithm, in this way underlining its universality. Finally, one may already have wondered where the apparently omnipresent *cosine tuning* discussed in the previous section comes from. As we will see through the concrete example of the sand scorpion, cosine tuning is a consequence of neuronal *interaction* and finds a simple explanation by means of linearization in the operational domain of the command neurons involved.

Though there is some previous work on special cases of cosine tuning in sensory systems and other species, both a neuronal model and a general context were missing until now. Here we like to mention that Bergenheim et al. (2000) show that PVA works for human muscle spindle afferents, Weber et al. (2006) display how population vectors operate for afferents recorded in the dorsal root ganglion (DRG), Bosco and Poppele (1993) indicate how PVA works for the dorsal spinocerebellar tract (DSCT), Kristan and Shaw (1997) have demonstrated cosine tuning in the leech, and Salinas and Abbott (1994) have analyzed the cricket cercal system with its purported wind-direction population vector. For a review of the early literature with a neat slant towards theoretical neuroscience the reader may profitably consult Abbott (1994).

Sand scorpion as pathfinder to PVA The sand scorpion *Paruroctonus mesaensis* is an ambush predator of insects and other scorpions, always hunting at night from a motionless rest position outside its burrow on the sand surface. It is a so-called "sit-and-wait", meaning here stand-and-wait, predator whose typical attack/defense position is shown in Fig. 4.

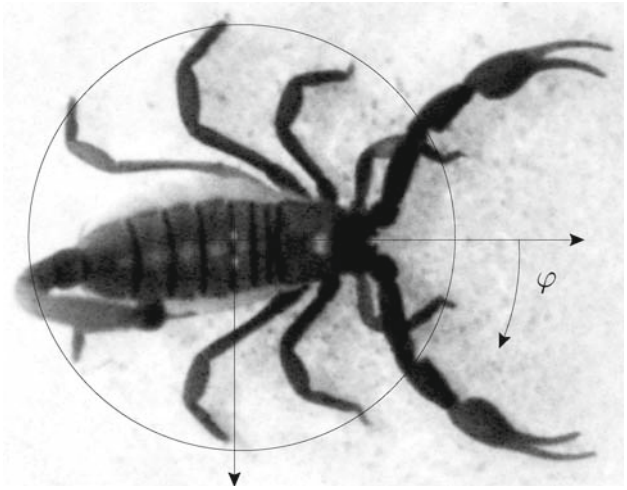

Fig. 4 Desert scorpion *Paruroctonus mesaensis* (about real size) as seen from above. It is in a defense position with its eight tarsi (feet) on a circle with radius $R \approx 2.5$ cm and its huge pedipalps in front. Tail and venom gland are ready for attack. The picture, due to Stürzl et al. (2000), is a negative of a scorpion that is fluorescent in the dark under the influence of ultraviolet light. The stimulus angle is $\varphi = \varphi_S$

The sand scorpion's typical habitat is the Mojave desert and it responds to surface (Rayleigh) waves generated by its prey, e.g., small insects walking on the sand surface. The tarsal detectors, the so-called basitarsal compound slit sensilla or BCSS, are located above the joint of the tarsus (foot) and basitarsus of each of the eight legs. They are extremely sensitive; for details we refer to Stürzl et al. (2000) and Brownell and van Hemmen (2001).

To localize prey the only information available to a sand scorpion is the arrival time difference between the BCSS due to the waves emanating from the stimulus, which is taken to be a point source, The BCSS are on a circle of radius $R \approx 2.5$ cm at angles $\gamma_k = \pm 18°, \pm 54°, \pm 90°$, and $\pm 140°$, where 0° is ahead; see Fig. 4. We label them by $1 \le k \le 8$ clockwise, starting with the right front leg. The Rayleigh wave generated by a stimulus at angle φ_S and distance r from the scorpion's center approximates a plane wave once $r \ge 8$ cm. For a given stimulus angle φ_S, the time difference $\Delta t(\varphi_S|\gamma_k, \gamma_l)$ between the arrival of a wave at two BCSS of tarsi at angles γ_k and γ_l is then

$$\Delta t(\varphi_S|\gamma_k, \gamma_l) \approx \frac{R}{v_R}\Big[\cos(\varphi_S - \gamma_l) - \cos(\varphi_S - \gamma_k)\Big] \qquad (2)$$

so that $\Delta t \in [-\Delta t_0, \Delta t_0]$ with $\Delta t_0 = 2R/v_R$ as the maximal time difference of about 1 ms. Here v_R is the velocity of Rayleigh waves in dry sand, which is surprisingly low: about 50 m/s. Hence 1 ms is the maximal duration of a wave passing by, which is still in the ordinary neuronal time range.

Balance of excitation and inhibition The next step in model formulation is to make an informed guess at the neuronal

mechanism that could transform time information into patterned neuronal activity in the scorpion's brain. While we know very little about the neuroanatomy of scorpion central nervous systems, we have fairly detailed studies of spiders (both are Arachnids) showing ring-shaped integrative neurons in the suboesophageal ganglion (SOG) where fiber tracts from their eight legs converge; see Brownell and van Hemmen (2001). Similarly, we know from behavioral observations of sand scorpions that vibration source localization requires integrative input from *multiple* receptors within the ring of eight, with receptors nearest and farthest away from the target having the greatest impact on accuracy (Brownell and Farley 1979); cf. Fig. 4.

Figure 5 shows a diagrammatic representation of interneuronal circuitry that meets the above requirements through conventional synaptic connectivity between a small set of interneurons. Central to its construction are eight excitatory command neurons and inhibitory partners which will evaluate the sensory input and eventually 'command' an appropriate motor output for rotation toward the target. Each BCSS, representing a direction γ_k, with $1 \leq k \leq 8$, excites its corresponding command interneuron and the associated inhibitory interneuron, both labeled by k. The latter also receives excitation from BCSS γ_{k-1} and γ_{k+1}, adjacent to γ_k, thus forming an *inhibitory triad* that will act with synaptic delay ($\Delta t_I = 0.7\,\mathrm{ms}$) to block the action of the command neuron coding for direction $\gamma_{\tilde{k}}$ *opposite* γ_k in the sensory field. Thus, for each command neuron encoding for turns in one direction (γ_k), the inhibitory triad antagonistic to it is centered and represented by $\tilde{k} = [(k+3) \bmod 8] + 1$.

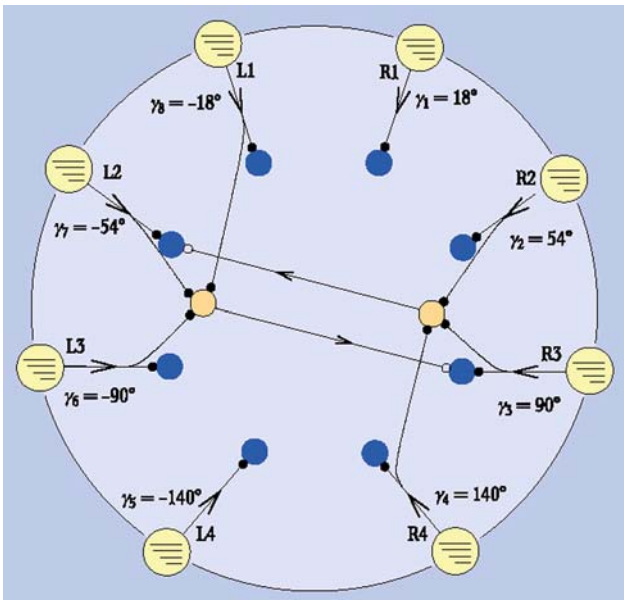

Fig. 5 Inhibitory triad model to account for vibration source localization in sand scorpions. The circular array of BCSS receptors (*outer circles*), at fixed angles γ_k relative to the sensory field center, innervate eight command neurons (*inner circles, dark*). Only two of the eight associated inhibitory neurons are shown (for clarity, only those corresponding to legs R3 and L2, i.e., k and $\tilde{k}$). Inhibitory and excitatory synapses are represented as open or darkened circles, respectively. This arrangement of neurons and interactions is hypothetical but consistent with other time-measuring circuits in vertebrates (Kapfer et al. 2002) and invertebrates (Barth 1985; Brownell and Polis 2001). Of course the scale is incorrect: The outer radius is $R \approx 2.5\,\mathrm{cm}$ whereas the inner one in the scorpion's brain (SOG) has a micron range. After Stürzl et al. (2000)

Population vector algorithm as actuator Let us now focus on Fig. 5. What are the command neurons going to do if a vibrational stimulus appears? They are in the direct neighborhood of the motor neurons that "command" the scorpion's leg muscles the animal has to use for turning and running to its prey once the latter becomes noticeable to the BCSS; say, once a year. Following Stürzl et al. (2000) and in the spirit of the population vector algorithm (PVA) as presented in the previous section, we now assign a unit vector $\boldsymbol{e}_k$ with direction γ_k to each command neuron k and propose that the animal's reaction is described by (1). That is, by the resultant vector population vector $\boldsymbol{n}$ made up from the individual contributions $\nu_k \boldsymbol{e}_k$ of the "committee" members γ_k, $1 \leq k \leq 8$, that fire at a rate ν_k. In this way the population vector algorithm functions *as a neuronal actuator*, a rather fascinating perspective.

The BCSS slits and, hence, neurons respond individually in dependence upon the intensity of the stimulus wave. Thus it may well be that instead of one committee we have a multiple of active committees of command neurons, each corresponding to a BCCS and patterned after Fig. 5. The ensuing arguments will not change, however, and our considerations are also valid in this more general context, which we will not discuss here. Instead we turn to a quality check.

The proof of the pudding is in the eating. Figure 6 shows a comparison between a healthy or lesioned scorpion's response to a vibrational stimulus and the predictions of the model (Stürzl et al. 2000). Sensory response of the BCSS is characterized by a very low threshold but the price the animal pays, so to speak, for this high sensitivity is that, though phase-locked, the spike response is somewhat stochastic so that all a realistic theory can predict is a probability distribution, represented by a corresponding density function. The latter appears as dark shading in Fig. 6. We see two things. First, the agreement is quite satisfying. Second, replacing the inhibitory triad of Fig. 5 by a single neuron gives an agreement that is far less good than that resulting from the triad. The key issue, however, is that the PVA is quite efficient as actuator of the animal's response originating directly (Brownell and van Hemmen 2001) from its motor system.

Cosine tuning Is there a cosine tuning of the individual command neurons and, if so, where does it come from? We have seen that tuning of individual command neurons stems from

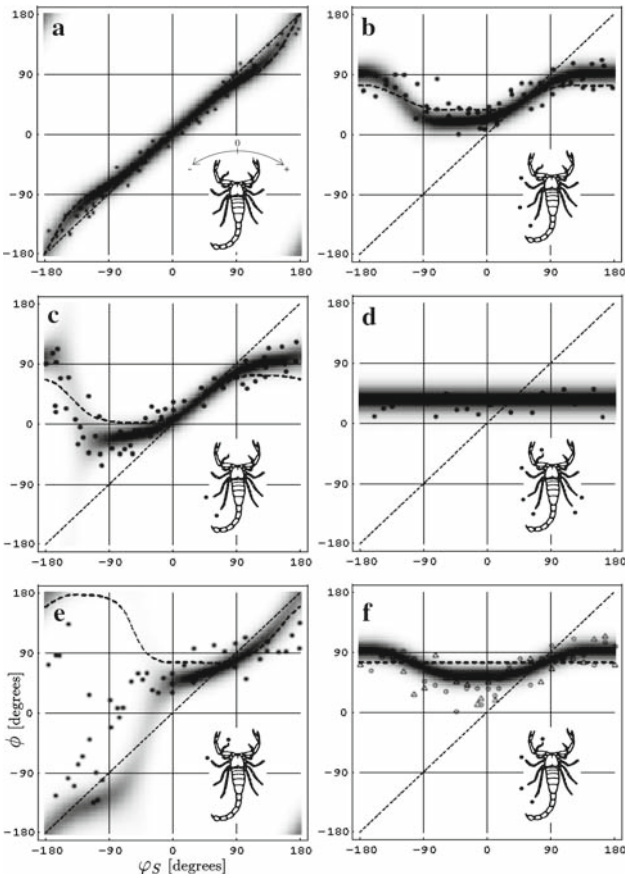

Fig. 6 Scorpion's response angle ϕ of (vertical axis) as a function of the stimulus angle φ_S (horizontal axis). **a** Systematic deviation, an undershooting, of the response of an intact animal that hardly ever manages the complete turn φ_S. **b–f** Ablated basitarsal compound slit sensilla (BCSS) are indicated by dots at the end of the tarsi (legs). Both the probability density $P(\phi)$ (*dark shadings*) and experimental points (*dots*) are indicated. Experimental data are due to Brownell and Farley (1979); see also Brownell (1977, 1984). If the inhibitory triad is replaced by a single inhibitory neuron, we find the *dashed line* as the mean response; the agreement with experiment is in general less good. Picture due to Stürzl et al. (2000)

the time differences between command neuron k's excitatory input and that from its inhibitory triad $\tilde{k}$ opposite to k. The leading time difference $\Delta t(\varphi_S|\gamma_k,\ \gamma_{\tilde{k}})$ as given by (2) has a cosine dependence upon the stimulus angle φ_S. It is convenient to compute the neuron's average number $\langle n_k\rangle$ of spikes as a function of the time difference Δt, the so-called tuning curve. Dividing by the duration of the time interval τ_S during which spike counting happens we obtain the mean "instantaneous" firing rate $\nu_k = \langle n_k\rangle/\tau_S$; admittedly this notion is a bit shaky since in counting spikes we cannot take the limit $\tau_S \to 0$. As we see in Fig. 7, it is a good approximation to take a linear Δt dependence,

$$\langle n_k\rangle(\Delta t) = a - b\,\Delta t, \tag{3}$$

with a and b positive constants for the *mean* number of spikes $\langle n_k\rangle$ in a time interval of length τ_S, the average (always

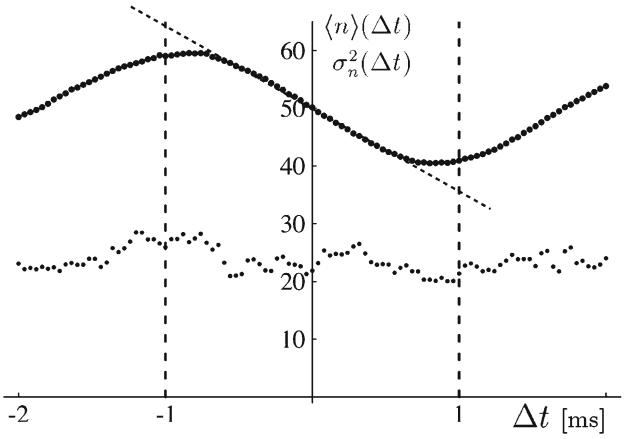

Fig. 7 Tuning curve (*top*), its linear approximation (dashed), and standard deviation (*bottom*) for a command neuron with $M = 2$ active neurons per BCSS; for the parameter values underlying the present plot resulting from an exact numerical evaluation with the neurons taken to be à la Hodgkin-Huxley; see Stürzl et al. (2000, Fig. 4). Within error bars the fit to the tuning curve is a cosine. The recording time τ_S was 500 ms, as in Brownell's experiments (Brownell and Farley 1979; Brownell 1984). The interval $[-1, 1]$ ms of the Δt axis between the vertical dashed lines being the physically accessible range, the linear approximation leading to (3) is fair

denoted by angular brackets) taken with respect to the probability distribution that we use to describe the neuronal response. The spontaneous rate ν_0 containing no directional information, we replace (Salinas and Abbott 1994) $\nu_k = n_k/\tau_S$ in (1) by $n_k - n_0$ with $n_0 = \nu_0\tau_S$ so as to get the "real" instantaneous firing rate ν_k.

Taking advantage of (1) and (3) we verify that $\langle\phi(\varphi_S)\rangle = \varphi_S$ if the legs and, thus, the angles γ_k were *equi*distributed according to $\gamma_k = -22.5° + k\,45°$ for $1 \le k \le 8$, and if the triad were the single neuron $\bar{k}$. Since $\langle\phi(\varphi_S)\rangle := \arg[\sum_k \langle n_k\rangle \exp(i\gamma_k)]$ where $\langle n_k\rangle$ is given by (5), we find

$$\langle\phi(\varphi_S)\rangle = \arg\left\{\sum_k [a + 2b\cos(\gamma_k - \varphi_S)]\,\mathrm{e}^{i\gamma_k}\right\} = \varphi_S \tag{4}$$

For realistic γ_k, an inhibitory triad, and dropping (3), we get a small but systematic deviation from φ_S as shown in Fig. 6a: for positive/negative φ_S the animal is off by about $\mp 10°$. We thus see that command neurons providing the sand scorpion's motor system with a population vector code they have generated themselves allow an even detailed explanation of the animal's prey capture performance.

We make a quick detour to what the above two-dimensional argument means for three-dimensional space-time. To this end we return to Eq. (1) but imagine that the animal aims at a stimulus it has detected in the direction $\boldsymbol{e}$. In three dimensions we replace the preferred directions γ_k simply by vectors $\boldsymbol{e}_k$; directions are always unit vectors. The instantaneous firing rates ν_k are supposed to be functions $f(\boldsymbol{e}\cdot\boldsymbol{e}_k)$ of the cosine of the angle between $\boldsymbol{e}$ and $\boldsymbol{e}_k$. Then PVA à la (1) reads

$$\boldsymbol{n} := v\boldsymbol{e} = \sum_{k=1}^{N} f(\boldsymbol{e}\cdot\boldsymbol{e}_k)\,\boldsymbol{e}_k. \tag{5}$$

Is, however, the right-hand side of (5) parallel to $\boldsymbol{e}$? In general it is not but let us, in view of the above results and the experimentally known cosine tuning, simply assume the function f is linear. For the moment we drop the constant vector $\sum_k \boldsymbol{e}_k$ and ask under what condition do we find

$$\sum_{k=1}^{N} b\,(\boldsymbol{e}\cdot\boldsymbol{e}_k)\,\boldsymbol{e}_k = v\boldsymbol{e}? \tag{6}$$

We cannot expect to get the exact equality in (6) but in view of our sand-scorpion example (4) it is plain that $(\boldsymbol{e}\cdot\boldsymbol{e}_k)$ may well do a decent job; see also Figs. 5 and 6. That is to say, from a practical point of view the weighted sum points in $\boldsymbol{e}$'s direction and we may wonder why this is so in general.

Cosine tuning revisited Since according to (3) the instantaneous firing rate ν_k is to fine approximation linear in Δt and (2) exhibits a cosine dependence upon φ_S we directly obtain a cosine tuning. To arrive at this conclusion three things have to be constantly borne in mind.

- First, it is an approximation – even for this very simple model.
- Second, the cosine dependence hinges on *neuronal interaction*. That is, in the example of Fig. 5 cosine tuning originates from the ring circuit of excitation-inhibition.
- Third, though detection may well depend on a millisecond precision of the sensory neurons including up to one or two nuclei in the brain, an actuator has to act, and acts, on the motor system. Hence all it needs is a *rate* instead of spike coding. Since the former is also much cheaper than the latter we see that brains drop temporal precision as quickly as possible. For example, a scorpion's SOG operates with millisecond precision even though its output is a firing rate. In addition, PVA hinges on rate coding, as is already evident from its very formulation (1).

How then should we look at (6) from a higher point of view? Let us imagine we have a cosine tuning of neurons that are dependent on an input stimulus with direction $\boldsymbol{e}$ and constitute an assembly of many, viz., N, participants. Furthermore, let us assume all their preferred directions $\boldsymbol{e}_k$ occur with about equal probability. For $N \gg 1$ the finite sum in the left-hand side of (6) can be approximated by an integral [due to the so-called random shooting or Monte Carlo evaluation of a multi-dimensional integral (Press et al. 2007)]. For a uniform distribution of directions we have to integrate over a unit circle in $d = 2$ and a unit sphere in $d = 3$ dimensions.

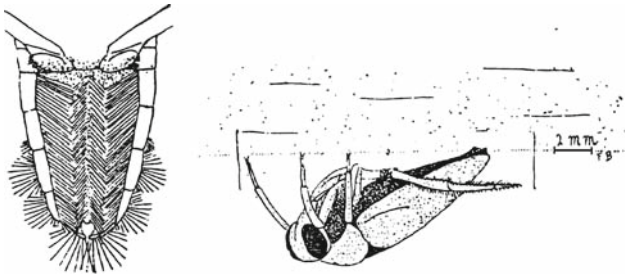

Fig. 8 *Left*: Abdominal hairs of the "ordinary" back swimmer *Notonecta glauca*, as seen from below. The two groups of hairs on the right and on the left function as detectors at the end of the body (Lang 1980). *Right*: Back swimmer hanging so to speak at the water surface. One sees one of the "rowing" legs and three of the four legs used for vibration detection. The scale bar on the right indicates 2 mm. The angles of the six legs are $\varphi_k = \pm 30°, \pm 90°, \pm 150°$ for the back swimmer studied here, viz., *Notonecta undulata*. Both pictures stem from C. Wesenberg-Lund, *Biologie der Süsswasserinsekten*, Springer, Berlin (1943) Figs. 115 and 116

For $d = 2$ we get $\langle\phi(\varphi_S)\rangle = \varphi_S$ through the very same symmetry argument as in (4). For $d = 3$ we take $\boldsymbol{e}$ instead of φ_S in the (x, y) plane, say $\varphi_S = 0$ parallel to the x-axis, and decompose the integral over the unit sphere into circles parallel to the (x, y) plane. Because of the underlying symmetry each circle gives a vector parallel to the x-axis and adding them all we get a vector parallel to $\boldsymbol{e}$, as desired. That is, for a homogeneous distribution of preferred directions in the motor system (Georgopoulos et al. 1988) and with $\boldsymbol{e}$ as a given token the PVA gives $\boldsymbol{e}$ as output—as it should. In the next section we will turn to the question of where the vectorial tokens may come from.

Back swimmer For a second example of the universality of PVA as a neuronal actuator we turn to the back swimmer, a surface-dwelling bug that spends much of its time hanging just beneath the surface of a quiet pond. It depends on a vibration sense to localize its prey, viz., insects that become trapped on the water surface. The vibrational frequency range is 20–150 Hz and the ripples may be as small as 1 μm. For details regarding various issues of its prey detection we refer to Murphey and Mendenhall (1973) and particularly Murphey (1973). Here too frequencies are so low that spike response is practically phase-locked, up to a stochastic scatter. The back swimmer is an insect with six legs, two of which it uses for "rowing". The receptors located at the tibio-tarsal joints of the remaining four legs together with two groups of abdominal receptors (i.e., hairs) at the end of the body (Fig. 8) provide the animal with the sensory input it needs for localizing its prey splashing at the water surface. That is, we take prey as a point source and the back swimmer as an animal living at the water surface and equipped with six, instead of eight, BCSS-like receptors.

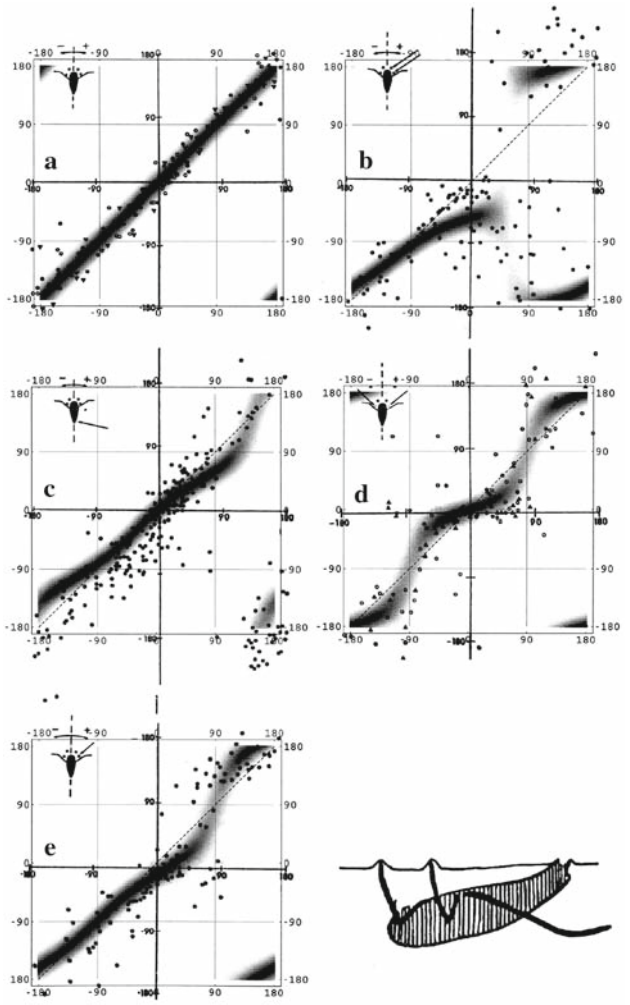

Fig. 9 Same as Fig. 6 but now for the back swimmer *Notonecta undulata* (in hunting position bottom right) with inhibition as specified by Murphey (1973). The horizontal axis is the input or stimulus one, the vertical axis indicates the response. Here **a** is for the back swimmer as such, this time heavy dots (top-left corner) indicating the positions of the front detectors, and **b**–**f** for lesioned animals with lesions indicated by an *arrow*. In addition, there are two groups of abdominal receptors at the very end. As we see, the agreement between experiment (*dots*) and theory (*dark shadings*) is at least as good as in Fig. 6. By reasons beyond our control several experimental points (*black dots*) are outside the plotting square $[-180°,\ 180°]^2$. By simply shifting them 360° upwards or downwards we see that the agreement becomes even better. Experimental data are due to Murphey and Mendenhall (1973, Figs. 2, 4b, 6) and Murphey (1973, Figs. 3 and 6)

Except for a few minor changes, we have used exactly the same model as before to explain a back swimmer's response to vibrational input and, lo and behold, Figure 9 shows that the model's description of the experimental data is at least as good as that of the sand scorpion in Fig. 6. This underlines the universality of the model and, more importantly in the present context, that of the population vector algorithm as a neuronal actuator.

4 Population vector code and what a map is good for

Equation (1) tells us that the "population vector" $\boldsymbol{n} := \nu \boldsymbol{e}$ is a vector sum of N constituents, viz., $\nu_i\ \boldsymbol{e}_i$ with $1 \leq i \leq N$. The vector $\boldsymbol{n}$ encodes the direction $\boldsymbol{e}$ of movement resulting from the assembly of N motor neurons while ν, its length, is proportional to the instantaneous speed of the drawing motion we focus on. The equation as such looks like a triviality but as a *mathematical* description of neurobiological reality it is not. Quite to the contrary, over the years it has turned out that the population vector as a resultant of motor action is universally valid. That is, it is a universal (van Hemmen 2007). Here we suggest that this universality may well extend beyond the motor system it has been devised for and that the population vector algorithm functions as a generally valid neuronal actuator.

Pondering about the sense of a population vector as a geometric universal in conjunction with the preferred directions $\boldsymbol{e}_i$, the cosine tuning, and the population vector algorithm (1) associated with all this, and despite its appealing function as neuronal actuator, we are nevertheless left with the puzzling question of where the vectorial tokens $\boldsymbol{e}_i$ as input come from and whether there is a still deeper meaning to the vector algorithm as such.

To see how we could answer these closely related questions we return to where it all came from, viz., the *maps* as neuronal representations of the outside sensory world and underlying the vector construction as such. The sand scorpion of Sect. 3 provides us with one of the simplest examples of a 'map' in that, once a stimulus is there, the "committee" of $N = 8$ command neurons in action, with their preferred directions $\boldsymbol{e}_k$ and $1 \leq k \leq N = 8$, effectively constitutes a map.

So we can ask (van Hemmen 2006): What is a neuronal map, how does it arise (a nature or nurture question), and what is it good for? A map as such is a representation of the outside sensory world in space-time, i.e., in space *and* time. Space-time consists of vector quantities. Of course one often has *additional* properties on top of space-time such as orientation in primary visual cortex of higher vertebrates but this we can, and will, skip here, just pointing out that time reappears for instance in the direction preference of V1 neurons. The point is not to hunt for complications but to exhibit general principles.

In Sect. 3, we have analyzed in detail two examples that were so simple that we could see at every stage what was happening. For quite a while the barn owl's azimuthal sound localization performed by the neurons in the laminar nucleus provided neurobiology with "the" example of a map (Konishi 1993, 2003) for which a complete theory (Gerstner et al. 1996; Kempter et al. 2001; van Hemmen 2001; Leibold and van Hemmen 2002) mathematically explaining it exists. For azimuthal sound localization in mammals the message is the

same but the mechanisms are different (Brand et al. 2002; Kapfer et al. 2002; McAlpine and Grothe 2003; Leibold and van Hemmen 2005). Interestingly, assigning to a map neuron k in the barn owl's laminar nucleus the encoded direction $\boldsymbol{e}_k$ in space, and taking the sum (1) over all map neurons, one finds the azimuthal direction the barn owl adopts (C. Leibold 2007 private communication). The laminar map is consistent with the principles of the population vector.

Space–time is vectorial. We therefore hypothesize that part of the answer to the question of 'What a neuronal map is good for?' is that neuronal maps as spatio-temporal representations of the outside world provide an animal's brain with vectorial input originating from its sensory modalities. The output of this map population is in the same vector form found in the motor system. Principles of linearity and cosine projection are the same in sensory and motor systems. From the perspective of control systems, this is an efficient strategy, eliminating the need for a transformation between the two. This type of design may also have significance in the future design of intelligent machines.

Acknowledgment The authors thank Wolfgang Stürzl for the simulations leading to Fig. 9.

References

Abbott LF (1994) Decoding neuronal firing and modelling neural networks. Q Rev Biophys 27:291–331

Averbeck BB, Latham PE, Pouget A (2006) Neural correlations, population coding, and computation. Nat Neurosci 6:358–366

Barth FG (ed) (1985) Neurobiology of arachnids. Springer, Berlin

Bergenheim M, Ribot-Ciscar E, Roll JP (2000) Proprioceptive population coding of two-dimensional limb movements in humans: I. Muscle spindle feedback during spatially oriented movements. Exp Brain Res 134:301–310

Bosco G, Poppele RE (1993) Broad directional tuning in spinal projections to the cerebellum. J Neurophysiol 70:863–866

Brand A, Behrend O, Marquardt T, McAlpine D, Grothe B (2002) Precise inhibition is essential for microsecond interaural time difference coding. Nature 417:543–547

Brownell PH (1977) Compressional and surface waves in sand: used by desert scorpions to locate prey. Science 1977:479–482

Brownell PH (1984) Prey detection by the sand scorpion. Sci Am 251(6):94–105

Brownell PH, Farley RD (1979) Detection of vibrations in sand by tarsal sense organs of the nocturnal scorpion *Paruroctonus mesaensis*. J Comp Physiol 131:23–30; Orientation to vibrations in sand by the nocturnal scorpion *Paruroctonus mesaensis*: mechanism of target localization. J Comp Physiol 131:31–38

Brownell PH, van Hemmen JL (2001) Vibration sensitivity and a computational theory for prey-localizing behavior in sand scorpions. Am Zool 41(5):1229–1240

Brownell PH, Polis G (eds) (2001) Scorpion biology and research. Oxford University Press, Oxford

Georgopoulos AP, Kalaska JF, Caminiti R, Massey JT (1982) On the relations between the direction of two-dimensional arm movements and cell discharge in primate motor cortex. J Neurosci 2:1527–1537

Georgopoulos AP, Caminiti R, Kalaska JF, Massey JT (1983) Spatial coding of movement: a hypothesis concerning the coding of movement direction by motor cortical populations. Exp Brain Res Suppl 7:327–336

Georgopoulos AP, Kalaska JF, Crutcher MD, Caminiti R, Massey JT (1984) The representation of movement direction in the motor cortex: single cell and population studies. In: Edelman GM, Goll WE, Cowan WM (eds) Dynamic aspects of neocortical function. Neurosciences Research Foundation, New York, pp 501–524

Georgopoulos AP, Kettner RE, Schwartz AB (1988) Primate motor cortex and free arm movements to visual targets in three-dimensional space. II. Coding of the direction of movement by a neuronal population. J Neurosci 8:2928–2937

Georgopoulos AP, Schwartz AB, Kettner RE (1986) Neuronal population coding of movement direction. Science 233:1416–1419

Gerstner W, Kempter R, van Hemmen JL, Wagner H (1996) A neuronal learning rule for sub-millisecond temporal coding. Nature 383:76–78

Hebb DO (1949) The organization of behavior. Wiley, New York

Helms Tillery SI, Flanders M, Soechting JF (1991) A coordinate system for the synthesis of visual and kinesthetic information. J Neurosci 11:770–778

van Hemmen JL (2001) Theory of synaptic plasticity. In: Moss F, Gielen S (eds) Handbook of biological physics, vol 4: neuro-informatics, neural modelling. Elsevier, Amsterdam, pp 771–823

van Hemmen JL (2006) What is a neuronal map, how does it arise, and what is it good for? In: van Hemmen and Sejnowski (2006), pp 83–102

van Hemmen JL (2007) Biology and mathematics: a fruitful merger of two cultures. Biol Cybern 97:1–3

van Hemmen JL, Sejnowski TJ (eds) (2006) 23 Problems in systems neuroscience.. Oxford University Press, New York

Johnson MT, Ebner TJ (2000) Processing of multiple kinematic signals in the cerebellum and motor cortices. Brain Res Rev 33:155–168

Kalaska JF, Caminiti R, Georgopoulos AP (1983) Cortical mechanisms related to the direction of two-dimensional arm movements: relations in parietal area 5 and comparison with motor cortex. Exp Brain Res 51:247–260

Kapfer C, Seidl AH, Schweizer H, Grothe B (2002) Experience-dependent refinement of inhibitory inputs to auditory coincidence-detector neurons. Nat Neurosci 5:247–253

Kempter R, Leibold C, Wagner H, van Hemmen JL (2001) Formation of temporal feature maps by axonal propagation of synaptic learning. Proc Natl Acad Sci USA 98:4166–4171

Konishi M (1993) Listening with two ears. Sci Am 268(4):34–41

Konishi M (2003) Coding of auditory space. Annu Rev Neurosci 26:31–55

Kristan WB Jr, Shaw BK (1997) Population coding and behavioral choice. Curr Opin Neurobiol 7:826–831

Kutz DF, Dannenberg W, Werner W, Hoffmann K-P (1997) Population coding of arm-movement-related neurons in and below the superior colliculus of Macaca mulatta. Biol Cybern 76:331–337

Lang HH (1980) Surface wave sensitivity of the back swimmer Notonecta glauca. Naturw 67:204–205

Leibold C, van Hemmen JL (2002) Mapping time. Biol Cybern 87:428–439

Leibold C, van Hemmen JL (2005) Spiking neurons learning phase delays: how mammals may develop auditory time-difference sensitivity. Phys Rev Lett 94:168102

Lewis JE (1999) Sensory processing and the network mechanisms for reading neuronal population codes. J Comp Physiol A 185:373–378

McAlpine D, Grothe B (2003) Sound localization and delay lines—do mammals fit the model? Trends Neurosci 26:347–350

Murphey RK, Mendenhall B (1973) Localization of receptors controlling orientation to prey by the back swimmer *Notonecta undulata*. J Comp Physiol A 84:19–30

Murphey RK (1973) Mutual inhibition and the organization of a non-visual orientation in *Notonecta*. J Comp Physiol A 84:31–40

Motter BC, Steinmetz MA, Duffy CJ, Mountcastle VB (1987) Functional properties of parietal visual neurons: mechanisms of directionality along a single axis. J Neurosci 7:154–176

Mountcastle VB (1998) The cerebral cortex.. Harvard University Press, Cambridge

Pellionisz A (1988) Tensorial aspects of the multidimensional massively parallel sensorimotor function of neuronal networks. In: Pompeiano O, Allum JHJ (eds) Progress in brain research, vol 76. Elsevier, Amsterdam, pp 341–354

Press WH, Teukolsky SA, Vetterling WT, Flannery BP (2007) Numerical recipes, 3rd edn. Cambridge University Press, Cambridge

Reina GA, Moran DW, Schwartz AB (2001) On the relationship between joint angular velocity and motor cortical discharge during reaching. J Neurophysiol 85:2576–2589

Salinas E, Abbott LF (1994) Vector reconstruction from firing rates. J Comput Neurosci 1:89–107

Schwartz AB (1992) Motor cortical activity during drawing movements: single-unit activity during sinusoid tracing. J Neurophysiol 68:528–541

Schwartz AB (1994) Direct cortical representation of drawing. Science 265:540–542

Schwartz AB (2007) Useful signals from motor cortex. J Physiol 579:581–601

Schwartz AB, Kettner RE, Georgopoulos AP (1988) Primate motor cortex and free arm movements to visual targets in three-dimensional space. I. Relations between single cell discharge and direction of movement. J Neurosci 8:2913–2927

Seung HS, Sompolinsky H (1993) Simple models for reading neuronal population codes. Proc Natl Acad Sci USA 90:10749–10753

Soechting JF (1989) Elements of coordinated arm movements in three-dimensional space. In: Wallace SA (eds) Perspectives on the coordination of Movement. North-Holland, Amsterdam, pp 47–83

Soechting JF, Flanders M (1991a) Arm movements in 3-dimensional space: Computation, theory, and observation. Exerc Sports Sci Rev 19:389–418

Soechting JF, Flanders M (1991b) Deducing central algorithms of arm movement control from kinematics. In: Humphrey DR, Freund H-J (eds) Motor control: concepts and issues. Wiley, New York, pp 293–306

Stürzl W, Kempter R, van Hemmen JL (2000) Theory of arachnid prey localization. Phys Rev Lett 84:5668–5671

Taylor DM, Helms Tillery SI, Schwartz AB (2002) Direct cortical control of 3D neuroprosthetic devices. Science 296:1829–1832

Turner RS, Anderson ME (1997) Pallidal discharge related to the kinematics of reaching movements in two dimensions. J Neurophysiol 77:1051–1074

Weber DJ, Stein RB, Everaert DG, Prochazka A (2006) Decoding sensory feedback from firing rates of afferent ensembles recorded in cat dorsal root ganglia in normal locomotion. IEEE Trans Neural Syst Rehabil Eng 14:240–243

Zhang K, Sejnowski TJ (1999) Neuronal tuning: to sharpen or broaden? Neural Comp NC 11:75–84